Molecular Twisting and Relaxation in the Excited State of Triarylpyrylium Cations

Darius Abramavicius,[†] Vidas Gulbinas,[†] Leonas Valkunas,[†] Ying-Jen Shiu,[‡] Kuo Kan Liang,[‡] Michitoshi Hayashi,*[,§] and Sheng Hsien Lin[‡]

Institute of Physics, A. Gostauto 12, Vilnius, 2600, Lithuania, Institute of Atomic and Molecular Sciences, Academia Sinica, Taipei, Taiwan, and Center of Condensed Matter Sciences, National Taiwan University, Taipei, Taiwan

Received: March 19, 2002; In Final Form: July 25, 2002

Excited-state twisting and relaxation of triarylpyrylium cations with various substituents attached to different parts of the molecule were studied by means of femtosecond pump−probe absorption spectroscopy and modeled numerically. The model was based on calculations of the population evolution on the excited- and ground-state potential surfaces, which are significantly different for nonstabilized and stabilized states because of the essential angular dependence of the stabilization energy. The modeling shows that a broad population distribution along the twisting angle in the ground state is transferred to the excited state, causing strong fluorescence broadening, while competition between the excited-state twisting and solvation determines a subsequent reaction path. The internal conversion rate is determined by the energy gap law and, depending on the attached substituents, is governed either by twisting or by solvation processes.

Introduction

Photoizomerization or molecular twisting is one of the puzzle processes of the molecular photoreactions in liquids. This process is usually considered as the relative rotation of the moieties of complex molecules at a substantial angle around a particular molecular bond.[1] The absorption and emission spectra, as well as radiative/nonradiative internal conversion rates, are functionally dependent on the twisting angle. In addition, substantial charge redistribution simultaneously with the molecular twisting takes place in some molecules, resulting in the so-called twisting-induced charge transfer (TICT) reaction.[2] For characterization of the TICT reaction, the evolution in a two-dimensional space related to the main reaction coordinates—the twisting angle and the charge redistribution inside the molecule—has to be taken into consideration.[3,4] Relaxation of other nonoverdamped higher-frequency intramolecular vibrations and reorganization of the solvent shell are usually either ignored or considered as independent of the system position along the main reaction coordinate. Most of the spectroscopic properties of molecules and the twisting reaction dynamics might be quite well explained within the framework of this approach. However, the twisting motion and the intramolecular charge transfer should be coupled with the rearrangement of the solvent shell and with other intramolecular vibrations. The latter degrees of freedom have also to be taken into account for the quantitative description of the TICT reactions.

The triarylpyrylium cations (see Figure 1) are good model compounds for detailed studies of the TICT reaction dynamics. By changing substituents attached to different parts of the molecule and varying the solvent viscosity, one can modulate the twisting rate providing valuable information about the processes responsible for the reaction control. Semiempirical quantum chemical calculations demonstrated that the dihedral angle θ between the pyrylium core and the phenyl group in the para position is equal to 30° in the equilibrium state, while it approaches 90° in the electronically excited state.[5] It was also

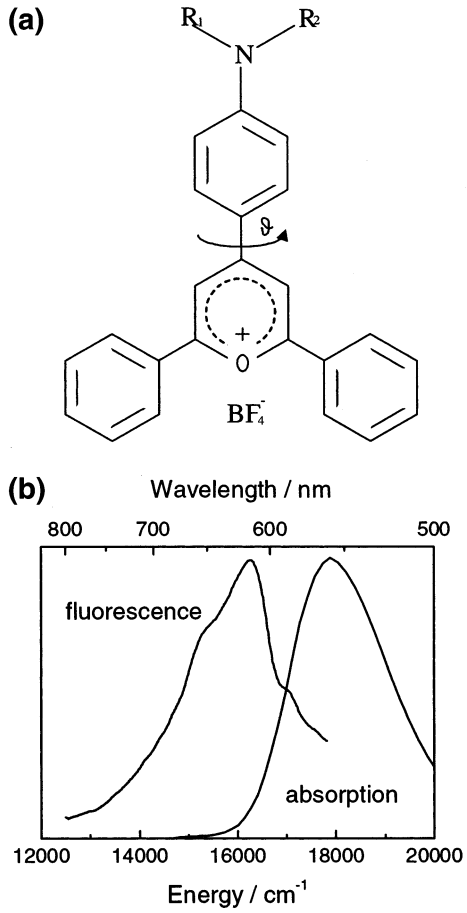

Figure 1. The structural formula (a) of triarylpyrylium cations and (b) absorption and fluorescence spectra of P_{1-12} in ethanol.

[†] Institute of Physics.
[‡] Academia Sinica.
[§] National Taiwan University.

10.1021/jp025788h CCC: $22.00
Published on Web 08/23/2002

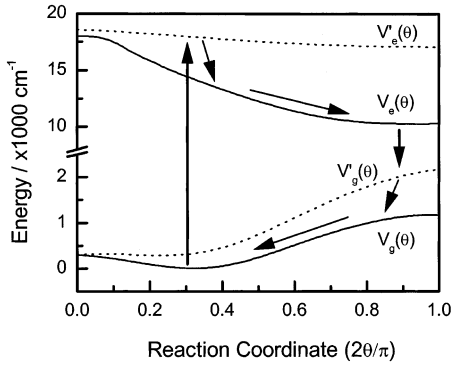

Figure 2. The scheme of the TICT relaxation demonstrating the energy potential dependence on the twisting angle. Arrows indicate the optical excitation and subsequent paths of the reaction on the excited- and ground-state potential surfaces because of the solvation and molecular twisting.

predicted that the 90° state must be "dark" in the sense that the molecules do not absorb or emit light because the corresponding electronic transitions are forbidden.

The femtosecond fluorescence up-conversion and picosecond pump−probe absorption spectroscopic methods were recently used for studies of the relaxation dynamics in triarylpyrylium cations.[6] On the basis of the data obtained, the following scheme for the relaxation process was suggested (see Figure 2). According to this scheme, the processes related to photoexcitation and relaxation can be grouped into the following five stages: (a) solvation and population spreading in the excited state; (b) molecular twisting; (c) internal conversion; (d) relaxation to the optically active ground state; (e) equilibration in the ground state. According to this scheme, the molecule finds itself on a slope of the excited-state potential surface after the optically induced Franck−Condon transition when its solvation shell is not equilibrated yet. The solvent rearrangement is assumed to be the fastest process causing the fast fluorescence shift. At the same time, the molecular twisting takes place leading to the fast fluorescence decay. The temporal evolution of the fluorescence decay has been related to the excited-state depopulation via an internal conversion and to the loss of the fluorescence oscillator strength when a molecule approaches the "dark" state. The internal conversion rate increases for the angles larger than 30° and becomes the fastest at 90°. After the internal conversion, the molecule finds itself in a nonrelaxed ground state characterized by a red-shifted absorption band. Molecular stabilization in the ground state is the final process in this sequence. The rates of different stages were determined from the analysis of time-resolved spectroscopic data obtained by fluorescence and pump−probe absorption measurements.

Though the principal relaxation scheme was determined, some important aspects of the relaxation process still remain obscure. The main problem under consideration is related to a very broad fluorescence (and stimulated emission) spectrum, extending from the absorption band located at ca. 550 nm to the near-infrared spectral region. Neither solvation nor molecular twisting on the relatively flat potential surfaces[5] could explain such strong broadening of the spectrum. Relatively low time resolution of the pump−probe experiments[6] (2 ps) was not sufficient to determine the very initial stages of the spectrum evolution. Though fluorescence investigations were performed with much higher time resolution, the excitation wavelength was too short (396 nm) in this case and more than 0.7 eV of the excess energy was supplied to the molecule by the absorbed light quantum.

To focus on the unsolved questions of the excited-state twisting and relaxation of triarylpyrylium cations, femtosecond absorption pump−probe experiments, together with the corresponding modeling of the processes, are presented in this paper. A more elaborated relaxation scheme is developed to explain the reaction dynamics, which is shown to be rather different for molecules with different substituents attached to them. The influence of the environment appears to be crucial in the relaxation process.

Methodology

Experimental Approach. The experimental setup was based on the femtosecond Ti−sapphire laser (Coherent Mira model 900-F) pumped by the argon-ion laser. Generated pulses of the 90 fs duration, 82 MHz frequency, and 1W mean power were amplified in a regenerative amplifier (Coherent RegA model 9000), pumped by the same argon-ion laser. The amplification process reduced the pulse frequency down to 20 kHz and increased the pulse energy up to 5 μJ. Later the amplified pulses were split into two parts. One part was focused on the sapphire plate to generate the white light continuum and the second part was converted into the second harmonics, which was used to pump a parametric amplifier. The main part of the continuum was used as the seeding light for the parametric amplifier (Coherent model 9400), which generates light pulses with ca. 0.2 μJ pulse energy tunable in the 450−700 nm range. These pulses served as the pump light in the pump−probe spectrometer. The remaining part of the continuum was used as the probe light.

The registration part of the pump−probe spectrometer was based on a spectrograph (Oriel MS257) equipped with a CCD camera. The probe beam was split into two parts and focused on the sample, one beam together with the pump beam and another about 1 mm away. After passing the sample, both probe beams were focused on the slit of the spectrograph and registered by the CCD camera. The transient differential absorption spectrum was calculated from the ratio of the two probe beam energies measured at some particular delay. The energy ratio measured at negative delay time was used as a zero signal. The differential absorption spectra were usually measured every 100 fs. Later the spectra were recalculated to compensate the probe pulse chirp.

The triarylpyrylium cations were synthesized as described elsewhere.[6] The samples of triarylpyrylium cations in butanol and ethanol solutions were measured in floating cuvettes of the 1 mm thickness.

The following notations will be used in the paper: P_{1-1} = triarylpyrylium cation with R_1 and R_2 being H nuclei; P_{1-12} = triarylpyrylium cation with R_1 being H nuclei and R_2 being $C_{12}H_{25}$.

Model Description. The approach used for the description of the excitation relaxation process in triarylpyrylium cations is based on the assumption that the solvation and redistribution of the intramolecular vibration energy are much faster than the molecular twisting over the rotation angle θ. Thus, molecular geometry and the solvation shell are fully adapted to a particular twisting angle, and therefore, the entire relaxation picture can be well determined as a projection into a one-dimensional space related to this twisting angle. The system evolution along this coordinate is considered as the diffusive process. Thus, the following scheme (see Figure 2) is accepted: potential surfaces $V_g(\theta)$ and $V_e(\theta)$ correspond to the vibrationally relaxed and solvated ground and excited states, while $V'_g(\theta)$ and $V'_e(\theta)$ correspond to the nonstabilized Franck−Condon states created immediately after the corresponding vertical electronic transitions.

The equilibrium ground-state population, $n_g(\theta,t=\infty)$, corresponds to the Boltzmann distribution of the twisting angles on the ground-state potential surface $V_g(\theta)$. Thus, the ground-state absorption (GSA) spectrum may be determined as

$$\alpha_{GSA}(\omega,t=\infty) \propto \int_0^{\pi/2} \sigma(\theta) n_g(\theta,t=\infty) f_{GSA}(\omega,\omega_{GSA}(\theta))\, d\theta \quad (1)$$

where $\sigma(\theta)$ is the angle-dependent absorption cross section and $f_{GSA}(\omega,\omega_{GSA}(\theta))$ determines the line-shape function at a particular twisting angle θ, characterized by the transition frequency $\omega_{GSA}(\theta) = \hbar^{-1}(V'_e(\theta) - V_g(\theta))$. The line-shape function can be attributed to the inhomogeneous broadening of the absorption spectrum related to all other degrees of freedom except the twisting angle. It may be defined by the Gaussian function with the central frequency $\omega_{GSA}(\theta)$ and the width Δ:

$$f(\omega,\omega_{GSA}(\theta)) \propto \exp(-4 \ln 2\, (\omega - \omega_{GSA}(\theta))^2/\Delta^2) \quad (2)$$

The initial population in the excited state, $n_e(\theta,\omega_{ex},t=0)$, created by the short excitation pulse with the light frequency ω_{ex} can be determined as

$$n_e(\theta,\omega_{ex},t=0) \propto \sigma(\theta) n_g(\theta,t=\infty) f(\omega_{ex},\omega_{GSA}(\theta)) \quad (3)$$

If the width of the line-shape function, Δ, is small in comparison with the spectrum of the transition frequencies $\omega_{GSA}(\theta)$, then the excitation pulse creates a narrow angular distribution in the excited state. In the opposite case, that is, when Δ is large, the angular distribution in the excited state obeys a simple form that is independent of the excitation wavelength. Then the initial populations prepared by the excitation pulse can be expressed as

$$n_e(\theta,t=0) \propto \sigma(\theta) n_g(\theta,t=\infty)$$
$$n_g(\theta,t=0) = n_e(\theta,t=0) - n_g(\theta,t=\infty) \quad (4)$$

The spectrum of the transition frequencies $\omega_{GSA}(\theta)$ for triarylpyrylium cations related to the distribution of twisting angles may be obtained from the calculated potential surfaces by taking into account the Boltzmann distribution on the ground-state potential surface. Because of relatively flat potentials, the calculated spectrum is about 3 times narrower than the absorption spectrum. Therefore, the width $\Delta = 1650$ cm^{-1} of the line shape is required to reproduce the experimental absorption spectrum. This is an indication that the width of the absorption spectrum is determined by Δ and, thus, that the initial populations may be described by eq 4.

Evolution of the populations in the excited state, $n_e(\theta,t)$, and that in the ground state, $n_g(\theta,t)$, may be described by the following diffusion equations:[7]

$$\frac{\partial}{\partial t} n_g(\theta,t) = D_g \frac{\partial^2 n_g(\theta,t)}{\partial \theta^2} + \frac{D_g}{kT} \frac{\partial}{\partial \theta}\left(n_g(\theta,t) \frac{dV_g(\theta)}{d\theta} \right) + k_{nr}(\theta) n_e(\theta,t)$$

$$\frac{\partial}{\partial t} n_e(\theta,t) = D_e \frac{\partial^2 n_e(\theta,t)}{\partial \theta^2} + \frac{D_e}{kT} \frac{\partial}{\partial \theta}\left(n_e(\theta,t) \frac{dV_e(\theta)}{d\theta} \right) - k_{nr}(\theta) n_e(\theta,t) \quad (5)$$

where $k_{nr}(\theta)$ is the nonradiative transition rate constant and D_g and D_e are the diffusion coefficients for the molecular motion along the twisting coordinate in the ground and excited states, respectively. Hereafter, we assume that the population decay is predominantly determined by the nonradiative transition.

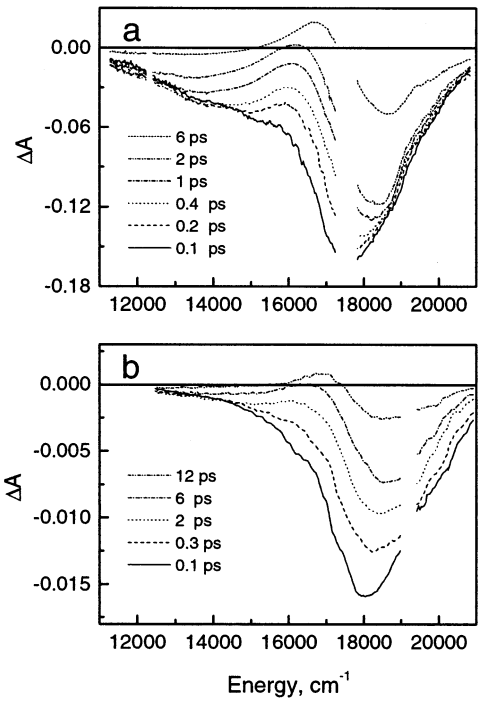

Figure 3. Transient differential absorption spectrum of (a) P_{1-12} in ethanol and (b) P_{1-1} in butanol excited at 17 540 and at 19 050 cm^{-1}, respectively, at a different probe delay after the pump pulse action.

The energy gap law is assumed to govern the nonradiative transition rate:[8]

$$k_{nr}(\theta) \propto \exp\left\{ -\frac{V_e(\theta) - V'_g(\theta)}{\hbar\Omega_0} \right\} \quad (6)$$

where Ω_0 is the frequency of the promoting mode. The time-dependent ground-state absorption spectrum of the excited system can be determined as

$$\alpha_{GSA}(\omega,t) \propto \int_0^{\pi/2} \sigma(\theta) n_g(\theta,t) f_{GSA}(\omega,\omega_{GSA}(\theta))\, d\theta \quad (7)$$

Similarly, the stimulated emission spectrum may be given by

$$\alpha_{SE}(\omega,t) \propto \int_0^{\pi/2} \sigma(\theta) n_{ex}(\theta,t) f_{SE}(\omega,\omega_{SE}(\theta))\, d\theta \quad (8)$$

where $f_{SE}(\omega,\omega_{SE}(\theta))$ is the line-shape function for the stimulated emission at a particular twisting angle characterized by the transition frequency $\omega_{SE}(\theta)$. It is evident that, by describing the shape of the emission line, $f_{SE}(\omega,\omega_{SE})$ can be chosen to be of the same shape as $f_{GSA}(\omega,\omega_{GSA})$ but with the different transition frequency: $\omega_{SE}(\theta) = \hbar^{-1}(V_e(\theta) - V'_g(\theta))$. The difference between ω_{GSA} and ω_{SE} is related to the stabilization energy. Therefore in the following, we will omit the indexes in the line-shape functions.

The transient differential absorption spectrum in the pump−probe experiments is determined by three constituents corresponding to the ground-state bleaching, stimulated emission, and excited-state absorption spectra. From the difference absorption spectra of triarylpyrylium cations[6] (see also Figure 3), it follows that the excited-state absorption in the particular spectral region under consideration is evidently much weaker than the first two components. By neglecting its input, one can

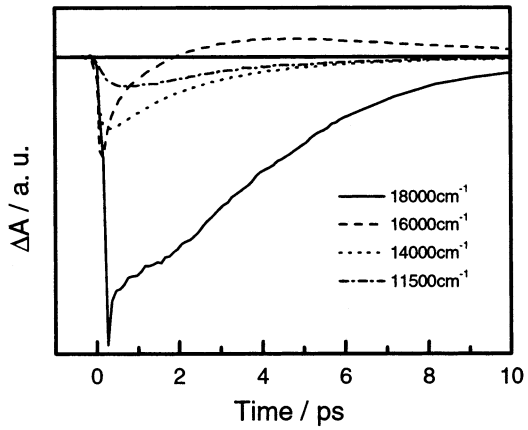

Figure 4. Transient absorption kinetics of P_{1-12} in ethanol at four different probing wavelengths.

determine the temporal evolution of the differential spectra as

$$\alpha_{p-p}(\omega,t) \propto \int_0^{\pi/2} d\theta\, \sigma(\theta)\{(n_g(\theta,t) - n_g(\theta,t=\infty))f(\omega,\omega_{GSA}) - n_{ex}(\theta,t)f(\omega,\omega_{SE})\} \quad (9)$$

The functional dependence of the absorption cross section $\sigma(\theta)$ on the rotation angle can be approximated from its limiting values at some particular angles. Indeed, the oscillator strength and thus the absorption cross section has to be a periodic function of the rotation angle with its maximal value at $\theta = 0$ and with the zero value at $\theta = \pi/2$. Therefore, the first harmonics of the Fourier series will be taken as the lowest-order approximation for the angular dependence, that is, it is assumed that

$$\sigma(\theta) = A\omega(1 + \cos(2\theta))/2 \quad (10)$$

where A is the constant related to the rate of the radiative decay and ω is the transition frequency.

Results and Discussion

The differential absorption spectra of P_{1-12} in ethanol and of P_{1-1} in butanol excited at 17 540 cm^{-1} (570 nm) and at 19 050 cm^{-1} (525 nm), respectively, are shown in Figure 3. According to the steady-state absorption (see Figure 1), the negative signal in the ca. 16 000−21 000 cm^{-1} region should be attributed mainly to the ground-state bleaching, while that at lower energies corresponds to the stimulated emission. At longer delay times, a positive signal appears at around 16 500 cm^{-1}, which should be related to molecules that already relaxed to the ground state but are still nonequilibrated. At the very initial time, the ground-state bleaching and the stimulated emission merge in a single band with a low-energy tail. During ca. 1 ps, the stimulated emission band shifts to low energies, and its intensity drops stronger than that of the ground-state bleaching. At long delay times, the stimulated emission band becomes very broad. It should be also noted that the stimulated emission band for the P_{1-1} solution in butanol is much weaker.

Figure 4 shows the transient absorption kinetics for P_{1-12} in ethanol at four different wavelengths, reflecting different aspects of the relaxation process. The absorption bleaching at 18 000 cm^{-1} has a fast decay component limited by the pulse duration. This fast component is absent on a short-wavelength side of the absorption bleaching band; thus, it should be attributed to the time evolution of the short-wavelength tail of the stimulated emission band. Contribution of the stimulated emission in this spectral region disappears at ca. 500 fs, and the decay rate drops down; however, it becomes faster again at ca. 2 ps. The differential absorption at 16 000 cm^{-1} reveals competition between the stimulated emission and the absorption of non-stabilized ground-state molecules. Because of the fast dynamic shift of the stimulated emission band, the transient absorption at this wavelength decays much faster than that in the absorption bleaching region. At ca. 2 ps delay time, the differential absorption turns out to be positive indicating that the absorption of the nonequilibrated ground-state molecules starts to prevail over the stimulated emission. The stimulated emission at 14 000 cm^{-1} appears with some delay and later decays with a time constant of ca. 3 ps. Similar behavior is observed at 11 500 cm^{-1} as well; however, the corresponding delay is slightly longer. The induced absorption at 16 000 cm^{-1} decays monotonically with ca. 5 ps time constant.

The temporal evolution of the transient absorption of the P_{1-12} solution in ethanol was calculated by means of the model presented above. Potential surfaces shown in Figure 2 were used for calculations. The stabilized ground-state potential surface, $V_g(\theta)$, and the potential of the Franck−Condon excited state, $V'_e(\theta)$, determining the absorption spectrum were chosen according to the semiempirical calculations of the molecule in the gas phase.[5] However, to reproduce the experimentally observed absorption spectrum, reduction of the energy gap by 10 700 cm^{-1} was assumed. The shapes of the potentials in the stabilized excited state, $V_e(\theta)$, and in the Franck−Condon ground state, $V'_g(\theta)$, which are the principle values determining the fluorescence spectrum and the population dynamics, were adjusted in the course of calculations. They were chosen to reproduce the steady-state fluorescence spectrum, the differential absorption spectrum, and its temporal evolution. In addition, the following motivations were also taken into account by determining the shapes of the potential surfaces mentioned above. The excited-state dipole moment increases with the twisting angle (14 D at 30° and 18 D at 90° according to Markovitsi et al.[5]); thus, the solvation energy should also increase at larger twisting angles. The stabilization energy in the ground state should follow roughly the same dependence. However, because the dipole moment of the molecules in the ground state is about 4 times smaller, the solvation energy and its angular dependence should be also weaker roughly by the same amount. Similar considerations are also valid regarding a part of the stabilization energy related to the intramolecular vibrational relaxation; the larger charge redistribution at larger twisting angles should induce larger nuclear displacements, thus causing larger energy of the vibrational relaxation. Bearing this in mind, we found the following empirical relationship between the surfaces to reproduce best the experimental results:

$$V_e(\theta) = V'_e(\theta) - V_{sol}(\theta/90) - 500 + 1000(\theta/90) \quad (11)$$

where

$$V_{sol}(x) = \frac{1}{2}\sum_{n=0}^{5} v_{sn}\left(1 + \tanh\left(\frac{x + d_{sn}}{s_{sn}}\right)\right) \quad (12)$$

and

$$V'_g(\theta) = 1000(\theta/90) + V_g(\theta) \quad (13)$$

The fitting parameters are presented in Table 1.

To describe the nonradiative relaxation according to eq 6, the frequency of the promoting mode, Ω_0, was assumed to be 1000 cm^{-1}. This can be associated with some mean value of the frequencies involved in the vibrational relaxation.[9] The

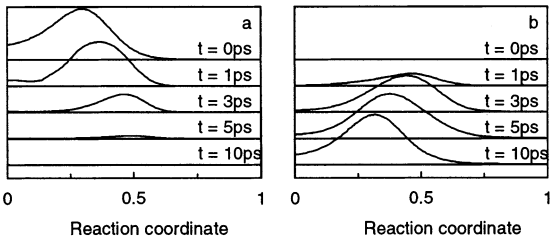

Figure 5. Calculated population evolution in the excited and ground states at different times for P_{1-12} in ethanol.

TABLE 1: The Fitting Parameters According to Eq 12

n	υ_{sn}	d_{sn}	s_{sn}
0	600	0.1	0.04
1	800	0.14	0.04
2	900	0.22	0.06
3	1800	0.33	0.15
4	1200	0.43	0.2
5	2000	0.6	0.2

vibrational frequencies of the molecule can be roughly grouped as follows: (1) Frequencies $\Omega \leq 100$ cm^{-1} are mainly related to the total motion of the molecule. (2) Motions of the separate benzene rings can be associated with $\Omega \leq 500$ cm^{-1}. (3) Vibrations inside the benzene ring (vibrations of the C−C bonds) are characterized by $\Omega \leq 1500$ cm^{-1}, while vibrations of the C−H bonds typically are close to 3000 cm^{-1}. Thus, the frequency of 1000 cm^{-1} used as the promoting mode correlates with the assumption that the internal conversion is related to the motion of the smaller groups of the molecule, that is, it may be associated with the bond that is participating in the molecular rotation. The amplitude of the nonradiative transition rate was determined from the fitting procedure. It was obtained that the nonradiative rate is 0.5 ps^{-1} at the rotation angle $\theta = 50°$.

The diffusion coefficients D_g and D_e were determined from the fitting procedure as well. The diffusion coefficient for the process under consideration depends on the solvent viscosity and on the size of rotating molecular fragments together with the solvation shells. Because of the difference in the dipole moments, the solvation shell is different in the ground and excited states resulting in the difference of the diffusion coefficients. Because of that, the diffusion coefficient should be larger in the ground state. The best agreement with the experimental data was obtained by assuming that $D_g = 0.05(\pi^2/4)$ and $D_e = 0.02(\pi^2/4)$ when the rotation coordinate is expressed in radians.

Figure 5 presents the calculated temporal evolution of the population density distribution on the ground- and excited-state potential surfaces shown in Figure 2. Because of the flatness of the potential surface in comparison with the thermal energy at room temperature, the equilibrium population in the ground state is initially spread in a wide range of twisting angles, from 0° to about 50°. This population distribution is transferred to the potential surface V'_e by the short pump pulse, and afterward a fast relaxation to the potential surface V_e takes place because of the solvation and vibrational relaxation. Thus, the stimulated emission and the population drift along the twisting coordinate toward the twisted state are related to the potential surface V_e. Following the energy gap law for the nonradiative relaxation (see eq 6), the internal conversion rate increases with the twisting angle and after reaching some particular twisting angle causes a fast relaxation of the system to the nonstabilized ground-state surface V'_g. The internal conversion rate for P_{1-12} in ethanol becomes fast in comparison with the population drift already

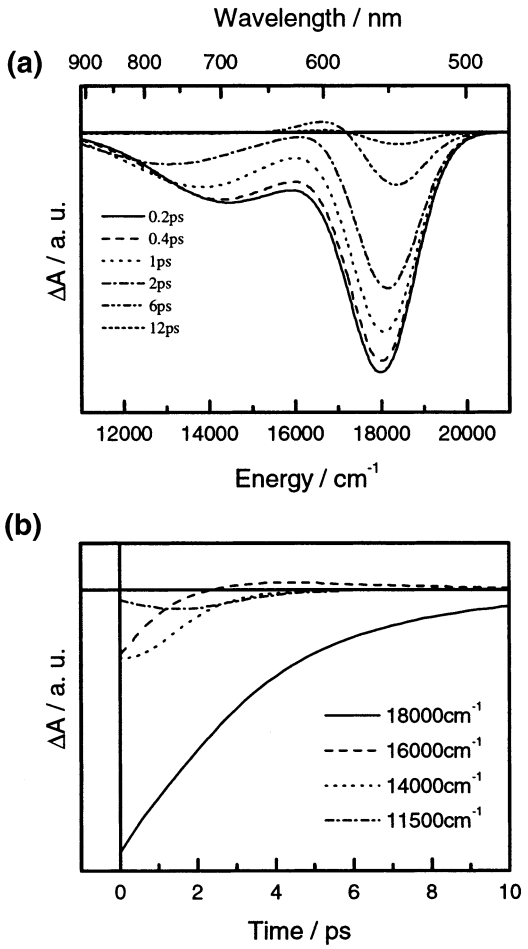

Figure 6. Time evolution of (a) the ΔA spectrum and (b) the ΔA kinetics at different wavelengths calculated for the system P_{1-12} in ethanol.

before reaching the twisted state, thus, the "dark state" corresponding to 90° of the twisting angle is not reached by the system. The calculated time evolution of the differential spectrum, ΔA, is shown in Figure 6. Sufficiently good agreement with the experimental data confirms the validity of the presumptions that were made in the model calculations.

The "dark state" of the molecule might be reached in the case when the twisting is faster than the internal conversion. This situation was clearly observed for pyrylium salt molecules without attached dodecyl chains in dichloromethane solution, in which only bleaching of the absorption band was evident at some particular delay time indicating that the molecules at this time have to be in the dark state.[6] A similar situation corresponds to the same triarylpyrylium salts in the butanol solution (see Figure 3b). The stimulated emission in this case is very weak, especially at longer delay times, which is a direct indication that molecules are twisted almost up to 90°. However, in contrast to the above-described model, the fluorescence spectrum is broadened and red-shifted much less than in the case of P_{1-12} molecules in ethanol. In this case, the assumption of the solvation process being significantly faster than the molecule twisting is not valid. Evidently, the molecules appear in the twisted configuration before the equilibration of the excited state. The scheme demonstrating competition between twisting and relaxation processes in this case is shown in Figure 7. There molecules reach the "dark state" before the solvation is attained. At this moment, the average transition dipole moment determining the stimulated transitions to the ground state is significantly reduced causing a very weak stimulated emission. Because the

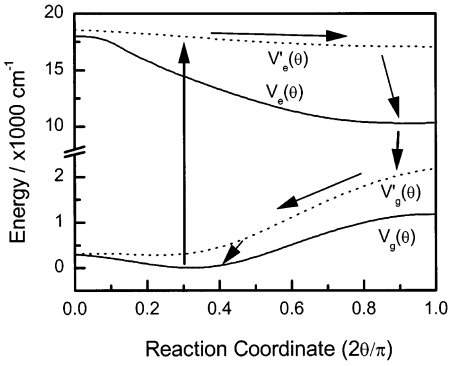

Figure 7. The TICT reaction scheme for P_{1-1} molecules in butanol. Arrows indicate the excitation and the expected paths of the relaxation. Here, an increase of the internal conversion is governed by the rate of the solvation process.

solvation is not finished yet, the energy gap remains relatively large resulting in the slow internal conversion. Thus, the molecules remain in the "dark state" for some time before the solvation process is over resulting in the reduction of the energy gap, which in its turn speeds up the internal conversion. Thus in contrast to the case of the P_{1-12} molecules described above, the internal conversion for P_{1-1} is controlled by the solvation rate rather than by twisting.

The twisting dynamics also requires some comments. One of the crucial problems is the validity of the classical diffusion description of the molecular motion. For the low-frequency overdamped molecular motions, the energies of those rotational modes are expected to be close to each other as compared to the thermal energy (at high temperatures at least), and therefore, the classical approach to the problem seems to be applicable. For higher-frequency vibrational modes, the applicability of this approach is disputable. The solvation process in general is very complex. However, when the solvent molecules are smaller than the typical extension of the motion under consideration, a large number of interaction events or collisions with the solvent molecules are expected. Therefore because of the central limit theorem, the average molecular motion can be expected to be Markovian and, thus, the description based on the Fokker−Planck equation is validated. However, for molecules without attached chains, the size of one of the rotating parts is comparable to the size of the solvent molecules. In this case, the total molecular twisting can happen even without any collision. The rotation process in this case cannot be described statistically. However, the memory, as well as quantum effects in the rotation process, can be implemented by the Monte Carlo method.

Summary

Investigation of the excited-state twisting and relaxation of triarylpyrylium cations in solutions by means of the femtosecond pump−probe absorption spectroscopy revealed the strong long-wavelength shift and broadening of the stimulated emission spectrum within the subpicosecond time domain. A model of four one-dimensional potential surfaces corresponding to non-stabilized and stabilized ground and excited states is proposed, and the system dynamics was modeled numerically. The modeling revealed that the observed spectroscopic peculiarities appear because of the stabilization energy dependence on the main reaction coordinate—the twisting angle. The stabilization energy increases for larger twisting angles causing a significant reduction of the energy gap and resulting in the broadening and long-wavelength shift of the fluorescence spectrum.

The modeling also revealed completion among three processes in the excited state—the molecular twisting, the excited-state stabilization, and the internal conversion. For molecules with substituents (P_{1-12}), the twisting is relatively slow and determines the time dependence of the energy gap and consequently the internal conversion rate. However, for molecules without substituents (P_{1-1}), the twisting process is much faster and the solvation appears to be slower limiting the reduction of the energy gap and the internal conversion rate.

According to these results, the conclusion is the following: the interaction of the system with the solvent is crucial in determining the spectroscopic properties, as well as the reaction path, during the twisting-induced excited-state relaxation. The competition of two main parameters, the solvation and the twisting rates, determines the path of the system relaxation. It follows that, by changing substituents attached to the molecule and the solvent, a different pattern of the reaction may be obtained, thus, enabling control of the ultrafast twisting process.

Acknowledgment. This research was supported by the Lithuanian-Latvian-Taiwan joint grant. Special thanks are given to Dimitra Markovitsi for the samples of pyrylium salts.

References and Notes

(1) Lippert, E.; Rettig, W.; Bonacic-Koutecky, V.; Heisel, F.; Miehé, J. A. In *Photophysics of Internal Twisting*; Prigogine, I., Rice, S. A., Eds.; Advances in Chemical Physics, Vol. 68; John Wiley & Sons: New York, 1987; pp 1−173.

(2) Rotkiewicz, K.; Grellman, K. H.; Grabowski, Z. R. *Chem. Phys. Lett.* **1973**, *19*, 315.

(3) Kim, H. J.; Hynes, J. T. J. *Photochem. Photobiol. A* **1997**, *105*, 337.

(4) Gulbinas, V.; Kodis, G.; Jursenas, S.; Valkunas, L.; Gruodis, A.; Mialocq, J.-C.; Pommeret, S.; Gustavsson, T. *J. Phys. Chem. A* **1999**, *103*, 3969.

(5) Markovitsi, D.; Sigal, H.; Ecoffet, C.; Millie, P.; Charra, F.; Fiorini, C.; Nunzi, J. M.; Strzelecka, H.; Veber, M.; Jallabert, C. *Chem. Phys.* **1994**, *182*, 69.

(6) Gulbinas, V.; Gustavsson, T.; Markovitsi, D.; Karpicz, R.; Veber, M. J. *J. Phys. Chem. A* **2000**, *104*, 5181.

(7) Toda, M.; Kubo, R.; Saito, N. *Statistical physics*; Springer−Verlag: Berlin, Heidelberg, New York, Tokyo, 1983; pp 1−2.

(8) Fain, B. *Irreversibilities in quantum mechanics*; Kluwer Academic Publishers: Dordrecht, Boston, London, 2000.

(9) Herzberg, G. *Molecular Spectroscopy and Molecular Structure*; van Nostrand Reinhold Company: New York, 1964−1966, reprint 1988−1991; p 3.